Effect of the oxidized and metallic phases of iron on the hydrodeoxygenation reaction of acetone

Key-words: Hydrodeoxygenation, Iron oxide, Nanomaterials.

Authors:

Pedro Becchelli de Moraes Nunes, IQ/Unicamp

Guilherme Boenny Strapasson, IQ/Unicamp

Profª. Drª. Daniela Zanchet (advisor), IQ/Unicamp

INTRODUCTION

One of the most widely known alternatives is the use and recovery of lignocellulosic biomass for the production of biofuels [1,2]. This recovery can present itself in the form of the rapid pyrolysis, which is extremely efficient in the production of bio-oil, a complex mixture of oxygenated compounds and represents a potential substitute for the production of diesel or gasoline derived from petroleum [3]. However, due to its physicochemical characteristics and especially its instability, due to the high content of oxygenated species, this mixture cannot be used directly as a fuel. In addition, the oxygenated compounds present in this complex mixture have high reactivity, making their storage difficult.

A bio-oil improvement process that has been widely studied is the catalytic hydrodeoxygenation (HDO) reaction. This reaction is conducted in a hydrogen-rich atmosphere in combination with a catalyst, leading to a reduction in the oxygen content through the cleavage of C-O bonds [4]. Due to the complexity of these compounds, a wide range of products can be formed, so that the HDO reaction can occur through several reaction mechanisms. The reaction scheme is extensive due to the wide variety of products, mechanisms and reaction sites that exist. Among the possible catalytic sites present in catalysts used in this reaction, there are: oxygen vacancy (OVS), Lewis acid (LAS), Bronsted acid (BAS), and metallic sites (MS) [5, 6, 7]. In addition to the routes through the aforementioned sites, there is also the direct deoxygenation route, which occurs through OVS by the reverse Mars-van Krevelen mechanism (rMvK) [8]. It is worth mentioning that all the aforementioned reaction pathways occur through the use of a heterogeneous catalyst, which depend on properties such as: its nature, phase (metallic or oxidized), particle size, specific surface area and crystalline structure.

In this context, the use of reduction/oxidation pre-treatments in reducible oxides allows obtaining catalysts with the coexistence of oxidized and metallic phases, inducing bifunctional mechanisms that can favor the formation of deoxygenated products. Leite [9] studied the nanometric Co_3O_4 and showed that different pre-treatments lead to the formation of onion-like particles, with cores and layers of different thicknesses and oxidation states, which impacts the exposed surface of the catalyst in a reaction environment and, therefore, the products formed. Another promising candidate for this reaction is iron oxide, as it makes it possible to study not only the effect of different oxidized (Fe_2O_3, Fe_3O_4 and FeO) and metallic (Fe) phases altogether, but also to understand the effect of their coexistence in the same particle.

In this manner, the present project evaluates the effects of the metallic and oxidized phases of iron on the HDO reaction of acetone, a model molecule for oxygenated derivatives containing ketone groups from biomass. The different phases of iron will be obtained through heat treatments in reducing and oxidizing atmospheres,

having as precursor the commercial nanometric iron (III) oxide (Fe2O3). The electronic and structural properties of these materials will be characterized and correlated with the catalytic data.

METHODOLOGY

Commercial nanometric (particle size <50 nm) iron(III) oxide (Fe_2O_3) acted as the HDO catalyst. In order to modify the catalyst's nature between the oxidized and metallic phases, different heat pretreatments were applied, such as reduction and oxidation of the precursor, using, respectively, reducing (H_2) and oxidizing (synthetic air) atmospheres at different temperature levels. In order to avoid extensive sintering of the iron catalyst, an excess of diluent in a 1:3 ratio was employed to mitigate the effect in question. It is worth noting that the diluent and the catalyst were used in the same range of granulometry, meaning that the oxide had to undergo a procedure of mechanical pressing and sieving until reaching a size between 100 and 200 mesh.

The catalytic reaction proceeded using a quartz reactor with a fixed bed, where a mixture containing 0.2 g (tests 1 and 2) or 0.6 g (tests 3 and 4) of the catalyst and 0.6 g or 1.8 g of diluent (α-alumina) is conditioned.

Pretreatments were applied for tests 2, 3 and 4: a thermal reduction to metallic Fe in tests 2 and 3, and a thermal reduction accompanied by a posterior oxidation for test 4. Both reductions were set at 550ºC, during the course of an hour, with the first one following through in a 10 ml/min H_2, 90 ml/min He atmosphere, and the other two in a 30 ml/min H2, 70 ml/min He atmosphere. Reduction temperatures of Fe_2O_3 were determined via H_2-TPR (Temperature Programmed Reduction), being set at 550ºC the FeO → Fe transition. The oxidation happened under a 100% atmosfere of synthetic air, at a 50 ml/min feed rate.

A 20 ml/min flow of He was used through a saturator containing acetone, in order to drag approximately 3.6 ml/min of it towards the reaction bed. A 76.4 ml/min flow of H_2 was also applied to the reaction medium, maintaining a proportion of approximately 21 mol of H_2 to 1 mol of acetone. The reaction was carried out at different temperature levels (100, 200, 300 and 400 °C) for tests 1 and 2, staying in each step for 30 minutes, and at a single 400ºC step for 180 minutes, pertaining to tests 3 and 4. In all four of them, a heating ramp of 10 °C/min was applied.

Following the tests, the identification and quantification of the HDO products happened by a GC/FID technique (gas chromatography by flame ionization analysis), while the post-reaction catalyst underwent a series of XRD analysis that will be discussed later on.

Once the compounds were quantified, the products were distributed in order to compare their selectivity as a function of the catalyst used. Another statistical data considered is the conversion of acetone, that is, how much of the starting material was converted into products.

RESULTS AND DISCUSSION

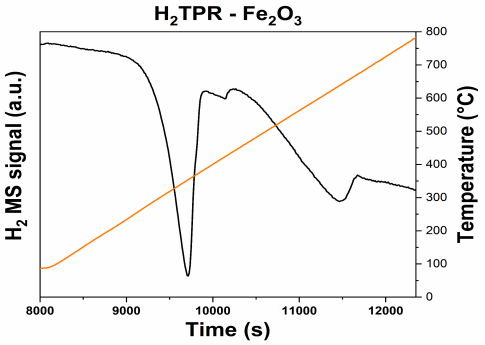

Figure 1 - H_2TPR of Fe_2O_3. Orange line corresponds to temperature variation, while the black line corresponds to H_2 consumption.

Examining the TPR above, it is possible to conclude that the best temperature to execute the oxide reduction to metallic iron lies around 550 ºC, in view of the lowering H_2 signal and, thus, increased consumption surrounding this specific temperature frame.

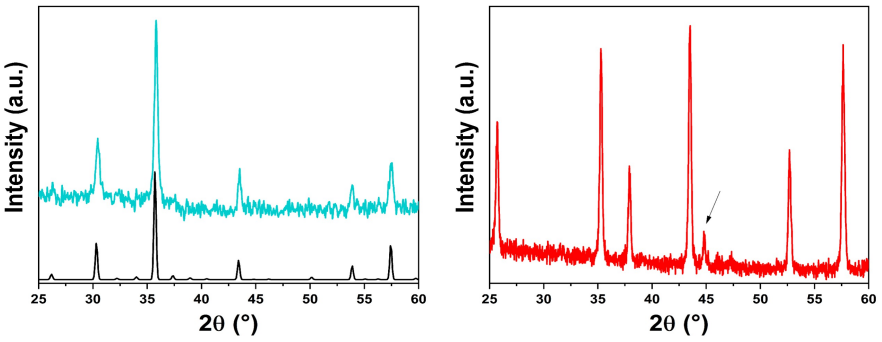

Figure 2 - (a) XRD analysis of commercial γ-Fe_2O_3 (light blue), in comparison to the literature reference from the ICSD database (black); (b) XRD analysis of the post-reaction sample (test 2) which received a reduction pretreatment. Cu wavelength was used in both (λ = 1.5148 A).

Figure 2a shows the comparison between a literature XRD of γ-Fe_2O_3 and an analysis of the commercial oxide used in this work. Matching peaks confirm the correspondence between data and the prevalence of maghemite in the utilized precursor. In contrast, Figure 2b brings information surrounding a second XRD relating to the post-reaction sample of test 2, which, beyond the HDO reaction itself, withstood a heat pretreatment of reduction. All peaks, except the one highlighted by an arrow, refer to the diluent α-alumina. The one peak around 45º relates to the metallic phase of iron, indicating success in the conduction of the treatment, which would be further confirmed after comparing the results from test 1 (pelletized commercial sample) with the results from tests 2 and 3 (reduced samples).

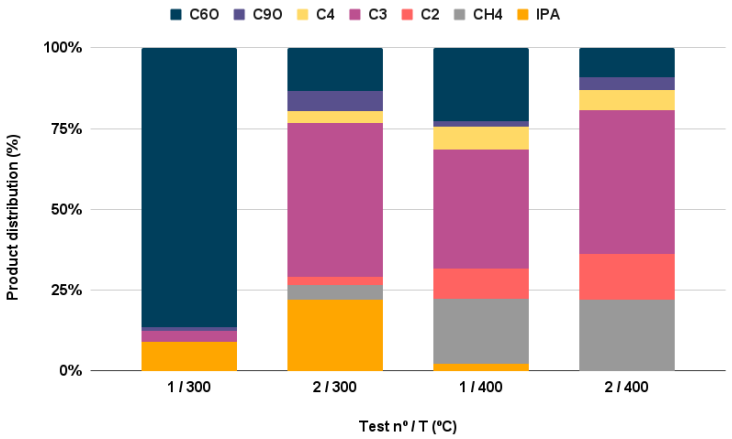

Figure 3 - Product distribution of acetone HDO at different oxide conditions (pelletized [T1] x pelletized and reduced [T2]) and different temperature ranges (300 ºC x 400 ºC).

Overall, the products of acetone HDO using Fe in its oxidized and metallic phases are quite similar, with the most reincident being methane (CH4), ethene and ethane (C2 on Fig. 3, C2E and C2A on Fig.3) , propene and propane (C3 on Fig. 3, C3E and C3A on Fig.4), butane and isobutene (C4), 2,6-dimethyl-4-heptanone (C6O) and 4-methyl-3-penten-2-one (C9O), with the last two ones being aldol condensation products.

It's noteworthy that, even though tests 1 and 2 were conducted at temperatures between 100 ºC and 400 ºC, the first two temperature stages present lower acetone conversion (as seen in Fig. 4) and less product

selectivity towards non-condensation products. This considered, only the distributions that occurred in 300º C or 400ºC will be considered for this present text.

When the 1/300 column of Fig.3 is put up against the 2/300 one, it's clear that the selectivity shifted from condensation products to more hydrodeoxygenated products when the precursor suffered a reducing pretreatment. Besides that, a 300 ºC distribution of a reduced sample is more similar to a 400 ºC distribution, whether it be reduced or non reduced, than it is to its non reduced 300 ºC counterpart, while preserving the same acetone conversion (about 14% in both cases), a phenomenon not seen when comparing both tests at 400 ºC (conversion diminishes from 33.2% to 22.8% when reduction happens beforehand, which may be explained by the catalyst's sintering properties).

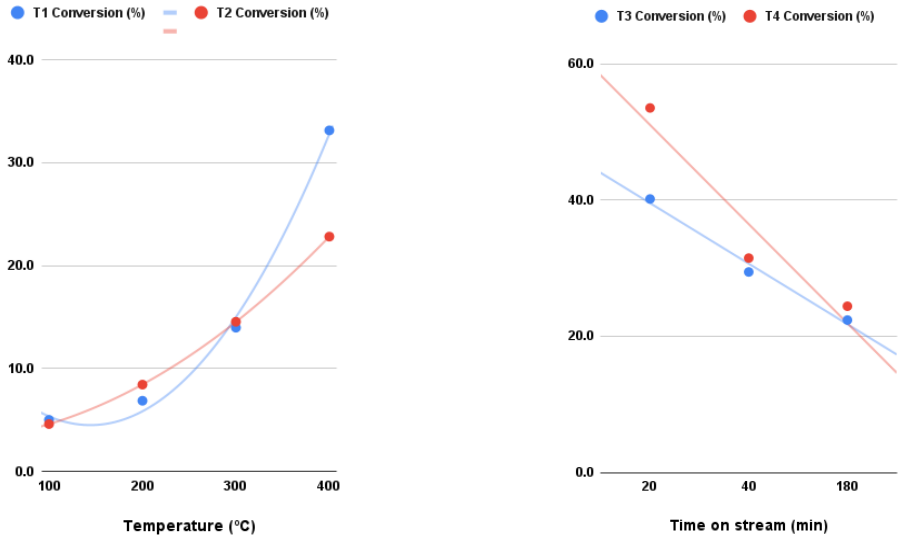

Figure 4 - (a) Acetone conversion (%) for tests 1 (blue) and 2 (red), in function of temperature (ºC); (b) (a) Acetone conversion (%) for tests 3 (blue) and 4 (red) at 400 ºC, in function of time on stream (min).

When working more specifically at 400º C level, with the reaction being left on stream for 3 hours, it is possible to observe more particular results. Figure 4b can be used to demonstrate the deactivation scenario of a catalyst, that is, the more time it spends on stream in a determined temperature level, the less it's able to convert acetone to any other product, being its most efficient and reactive during the 20 first minutes of reaction. Similarly, Figure 5 as a whole shows the increasing preference of condensation products formation as the reaction advances, while simultaneously exhibits the preference for C3 products formation, being it propane or propene.

Focusing on the catalysts themselves (test 3's endured a reduction pretreatment, while test 4's went through both a reduction and an oxidation procedure, which could create a core-shell structure [9]), the main distinction comes in the C3 class of products: while T3's catalyst seem to favor only propene, T4's favors both propene and propane, though the alkene still prevails. According to Leite [9], propene can be reached via dehydration of isopropanol and further reaction on a BA site, or through a direct reaction via a OV site, while propane is achieved by the hydrogenation of propene via a metallic site.

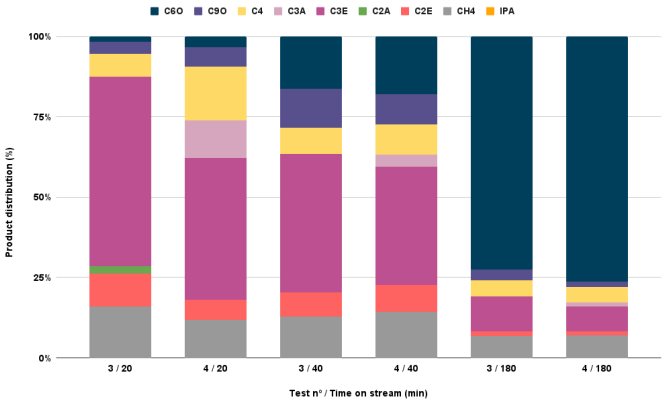

Figure 5 - Product distribution of acetone HDO at different oxide conditions (pelletized and reduced [T3] x pelletized, reduced and oxidized [T4]) and different times on stream (20 min x 40 min x 180 min).

CONCLUSIONS

Leaning on the test results obtained so far, in special the comparisons between T1's and T1's 300 ºC product selectivities and conversion rates, as well as the presence of a considerable amount of propane in T4's distribution, and the lack of it on T3, it can be concluded that significant changes may arise from the pretreatments applied, which would directly point to valorization and depreciation of the reaction sites contained by the catalyst.

Concerning the acetone conversion rates and condensation products formation, a coherent prediction of the circumstances around those events could be made as well. When the catalyst is the least active, the lower the conversion rate is and the more this type of product shows in significance compared to the others , which tends to happen in two instances: lower temperatures (<400 ºC without pretreatments, <300 ºC with at least a reduction treatment), and longer times on stream, contributing to deactivating the catalyst and its sites on a overall.

With this in view, it can be said that further testing needs to be done in order to gather more data and trace more parallels between the HDO results and the catalyst characteristics, including, but not limited to, more catalytic tests, while diversifying the variables involved (such as temperature, catalyst mass, oxidation circumstances, etc), XRD analysis of the oxidized samples or other samples from future tests, surface analysis by XPS and Py - FTIR Spectroscopy.

REFERENCES

[1] QIAN, Eika W.. **Pretreatment and Saccharification of Lignocellulosic Biomass**. In: TOJO, Seishu; HIRASAWA, Tadashi. Research Approaches to Sustainable Biomass Systems.Academic Press, 2014. Cap.7. p.181-204. DOI: doi.org/10.1016/B978-0-12-404609-2.00007-6.

[2] CARROLL, A., SOMERVILLE, C. **Cellulosic Biofuels.** Annual review of plant biology, 2008. 60. 165-82. 10.1146/annurev.arplant.043008.092125.

[3] MONTOYA, J. I.; CHEJNE-JANNA, F.; GARCIA-PEREZ, M. **Fast pyrolysis of biomass: A review of relevant aspects.: Part I:** Parametric study. Dyna rev.fac.nac.minas, Medellín , v. 82, n. 192, p. 239-248, Aug. 2015 . DOI: https://doi.org/10.15446/dyna.v82n192.44701

[4] MORTENSEN, P. M.; GRUNWALDT, J. D.; JENSEN, P. A.; KNUDSEN, K. G.; JENSEN, A. D. **A review of catalytic upgrading of bio-oil to engine fuels**. Applied Catalysis A: General, 2011. DOI: 10.1016/j.apcata.2011.08.046

[5] KIM, Soosan; KWON, Eilhann E.; KIM, Yong Tae; JUNG, Sungyup; KIM, Hyung Ju; HUBER, George W.; LEE, Jechan (2019). **Recent Advances in Hydrodeoxygenation of Biomass-Derived Oxygenates over Heterogeneous Catalysts**. Green Chemistry. 21. 3715–3743. 10.1039/C9GC01210A.

[6] YAN, Penghui; LI, Molly; KENNEDY, Eric; ADESINA, Adesoji; ZHAO, Guangyu; SETIAWAN, Adi; STOCKENHUBER, Michael. (2020). **The role of acid and metal sites in hydrodeoxygenation of guaiacol over Ni/Beta catalysts**. Catalysis Science & Technology. 10. 810-825. 10.1039/C9CY01970G.

[7] SUN**,** Junming; BAYLON, Rebecca A. L.; LIU, Changjun; MEI, Donghai; MARTIN, Kevin J.; VENKITASUBRAMANIAN, Padmesh; WANG, Yong. **Key Roles of Lewis Acid–Base Pairs on ZnxZryOz in Direct Ethanol/Acetone to Isobutene Conversion.** Journal of the American Chemical Society 2016 138 (2), 507-517 DOI: 10.1021/jacs.5b07401

[8] MIRONENKO, Alexander V.; VLACHOS, Dionisios G.; **Conjugation-Driven "Reverse Mars–van Krevelen"-Type Radical Mechanism for Low-Temperature C–O Bond Activation.** Journal of the American Chemical Society 2016 138 (26), 8104-8113 DOI: 10.1021/jacs.6b02871

[9] LEITE, D.S. **Efeito das fases metálica e oxidada do catalisador na hidrodesoxigenação de acetona**, Dissertação de mestrado, Instituto de Química - Universidade Estadual de Campinas, defendida em 21/02/2022.